Published in final edited form as:
Exp Neurol. 2012 September ; 237(1): 223–237. doi:10.1016/j.expneurol.2012.06.017.

Expression and Distribution of TRPV2 in Rat Brain

Thekkethil Prashant Nedungadi[1], **Mayurika Dutta**[1], **Chandra Sekhar Bathina**[1], **Michael J Caterina**[2], and **J. Thomas Cunningham**[1]

[1]Department of Integrative Physiology and Cardiovascular Research Institute, University of North Texas Health Science Center at Fort Worth, 3500 Camp Bowie Blvd, Fort Worth, TX, USA 76107

[2]Department of Biological Chemistry, Department of Neuroscience, Center for Sensory Biology, Johns Hopkins University School of Medicine, 725 N. Wolfe St. 408 Biophysics Building, Baltimore, MD, USA 21205

Abstract

Transient receptor potential (TRP) proteins are non-selective cation channels that mediate sensory transduction. The neuroanatomical localization and the physiological roles of isoform TRPV2 in the rodent brain are largely unknown. We report here the neuroanatomical distribution of TRPV2 in the adult male rat brain focusing on hypothalamus and hindbrain regions involved in osmoregulation, autonomic function and energy metabolism. For this we utilized immunohistochemistry combined with brighfield microscopy. In the forebrain, the densest immunostaining was seen in both the supraoptic nucleus (SON) and the magnocellular division of the paraventricular nucleus (PVN) of the hypothalamus. TRPV2 immunoreactivity was also seen in the organum vasculosum of the lamina terminalis, the median preoptic nucleus and the subfornical organ, in addition to the arcuate nucleus of the hypothalamus (ARH), the medial forebrain bundle, the cingulate cortex and the globus pallidus to name a few. In the hindbrain, intense staining was seen in the nucleus of the solitary tract, hypoglossal nucleus, nucleus ambiguous, and the rostral division of the ventrolateral medulla (RVLM) and some mild staining in the area prostrema. To ascertain the specificity of the TRPV2 antibody used in this paper, we compared the TRPV2 immunoreactivity of wildtype (WT) and knockout (KO) mouse brain tissue. Double immunostaining with arginine vasopressin (AVP) using confocal microscopy showed a high degree of colocalization of TRPV2 in the magnocellular SON and PVN. Using laser capture microdissection (LCM) we also show that AVP neurons in the SON contain TRPV2 mRNA. TRPV2 was also co-localized with dopamine beta hydroxylase (DBH) in the NTS and the RVLM of the hindbrain. Based on our results, TRPV2 may play an important role in several CNS networks that regulate body fluid homeostasis, autonomic function, and metabolism.

Keywords

vasopressin; supraoptic nucleus; nucleus of the solitary tract; brainstem; hypothalamus

*Correspondence to: J. Thomas Cunningham, Department of Integrative Physiology, University of North Texas Health Science Center at Fort Worth, 3500 Camp Bowie Blvd, Fort Worth, TX 76107, Phone: 817-735-5096, Fax: 817-735-5084, Tom.Cunningham@unthsc.edu.

Introduction

Ever since the first description and identification of Transient Receptor Protein (TRP) channels in Drosophila as a phototransducer, our understanding of the functions and structures of TRP channels has evolved and currently TRP channel proteins includes seven subfamilies (Moran, et al., 2011, Venkatachalam and Montell, 2007). A common functional aspect of TRP channels is their involvement in sensory transduction. The vanilloid subfamily of TRP channels (TRPV) is made up of six subtypes TRPV1-6 that are calcium permeable cationic channels responding by various degrees to thermal and mechanical stimulation (Caterina, et al., 1999, Hisanaga, et al., 2009). Functional studies indicate that TRPV channels participate in nociception (Caterina, et al., 2000, Davis, et al., 2000, Szallasi and Blumberg, 1999), myogenic tone (Knot and Nelson, 1995, Scotland, et al., 2004, Welsh, et al., 2002), mechanosensation (Christensen and Corey, 2007, Colbert, et al., 1997, Corey, 2003, Lin and Corey, 2005, O'Neil and Heller, 2005) and osmoregulation (Bourque, et al., 2007, Liedtke, 2006, Liedtke, et al., 2000, Sharif-Naeini, et al., 2008, Sudbury, et al., 2010).

TRPV2 was first identified based on its sequence homology with TRPV1 and characterized by its activation at high temperatures, with a threshold of approximately 52°C (Caterina, et al., 1999, Guler, et al., 2002). TRPV2 is extensively localized in the trigeminal ganglia (Ichikawa and Sugimoto, 2001, Park, et al., 2011), spinal cord (Caterina, et al., 1999, Lewinter, et al., 2004, Park, et al., 2011) and in the dorsal root ganglia (Caterina, et al., 1999, Park, et al., 2011). In these structures, TRPV2 is expressed most abundantly among a subpopulation of medium- to large-diameter neurons. Based on these and other findings, it had been speculated that TRPV2 was proposed to might be involved in thermal nociception and hyperalgesia. Yet, extensive characterization of mice lacking TRPV2 failed to reveal any deficits in nociception, either at baseline, or following nerve injury or inflammation (Park, et al., 2011). In addition to its thermal sensitivity, it has been shown that TRPV2 responds to mechanical stress in vascular smooth muscle cells(Muraki, et al., 2003) and cultured sensory neurons (Shibasaki, et al., 2010), where it may function as a mechanosensor. TRPV2 is also believed to play a role in osmotic cell swelling in murine aortic myocytes (Beech, et al., 2004, Muraki, et al., 2003) TRPV2 is expressed in the pancreatic ductal cells and the beta cells, as well as in MIN6 insulinoma cells (Hisanaga, et al., 2009, Kanzaki, et al., 1999). In beta cells, insulin-induced calcium entry is inhibited by shRNA knockdown of TRPV2 (Hisanaga, et al., 2009). TRPV2 has also been implicated in macrophage and prostate cancer cell chemotaxis (Link, et al., 2010, Monet, et al., 2009, Nagasawa, et al., 2007), as well as macrophage phagocytosis and cytokine release (Link, et al., 2010, Yamashiro, et al., 2010). In each of these contexts, only limited data are available which identify the mechanisms of activation or endogenous ligands, if any, for TRPV2. One common theme is that the activation of PI3 kinase appears to drive translocation of TRPV2 to the plasma membrane as well as its activation (Kanzaki, et al., 1999, Nagasawa, et al., 2007, Penna, et al., 2006).

There is little information on the expression and the function of TRPV2 in the rodent brain. Recently published work from our lab demonstrated co-existence of TRPV2 in vasopressin and oxytocin magnocellular neurons of the SON and PVN in an animal model of hyponatremia (Nedungadi, et al., 2012). Previous study on the neuroanatomical distribution of TRPV2-immunoreactivity in primate macaque brain identified TRPV2 to be highly restrictively localized to the hypothalamic paraventricular, suprachiasmatic, and supraoptic nucleus and colocalized with oxytocinergic and vasopressinergic neurons suggesting the possibility of a fundamental role for TRPV2 in mediating the activation of neurohypophysial neurons and possible involvement of TRPV2 in the hypothalamo-pituitary-adrenal axis (Wainwright, et al., 2004). The purpose of this study was to confirm and extend these observations by determining the anatomical localization of TRPV2 channels in the rat brain,

focusing on the hypothalamic and hindbrain regions by immunohistochemistry and laser capture microdissection.

Materials and Methods

Animals

Experiments were conducted on adult male Sprague-Dawley rats (250–350g, Charles River Laboratories, Inc., Wilmington, MA, USA). Rats were individually housed and maintained in a temperature-controlled (23°C) environment under a 12: 12h light/dark cycle with light onset at 0700h. Rats had *ad libitum* access to food and water. All experimental procedures were approved by the University of North Texas Health Science Center Institutional Animal Care and Use Committee according to the guidelines of the Public Health Service, the American Physiological Society, and the Society for Neuroscience. Wild-type (WT) and TRPV2 knockout (KO) mice (Park, et al., 2011) were bred and maintained in accordance with guidelines of the Johns Hopkins University Animal Care and Use Committee.

Immunohistochemistry

Rats (n=7) were deeply anesthetized with an intraperitoneal injection of thiobutabarbital (Inactin, Sigma, 100mg/kg) and perfused transcardially with 0.1M phosphate buffered saline (PBS) followed by 4% paraformaldehyde (PFA). Brains and pituitaries were removed, post-fixed in 4% PFA for 2h, and then transferred to 30% sucrose-PBS for 2–3 days until sunk. Forebrains and hindbrains were sectioned coronally at 40 μm and the pituitaries sectioned coronally at 20μm on a Leica cryostat. Four serial sets of coronal sections from each brain were placed in cryoprotectant (Watson, et al., 1986) and stored at −20°C in multiwall tissue culture plates until they were processed for immunohistochemistry (IHC). Pituitary sections were directly mounted onto gelatin coated slides and processed for IHC immediately after. TRPV2 KO and WT mice were deeply anesthetized with ketamine and xylazine (Park, et al., 2011). Perfusion and tissue preparation were conducted as in the rat. Coronal sections were cut at 40 μm for the hindbrain and the forebrain and placed in cryoprotectant until ready for use while the dorsal root ganglia was cut at 20 μm and directly mounted onto gelatin coated slides for IHC.

For each animal, a series of forebrain sections extending from the anterior olfactory nucleus to the caudal end of the arcuate nucleus of the hypothalamus and a series of hindbrain sections extending from the pyramidal decussation to the caudal midbrain were used for TRPV2 immunohistochemistry employing a peroxidase reaction. The primary antibody was raised against a synthetic peptide corresponding to amino acids 744–761 of rat vanilloid receptor like protein 2 (rabbit anti-TRPV2, Calbiochem, EMD Chemicals Inc. Gibbstown, NJ). Before incubation in the primary antibody, the sections were washed 4-8 times in PBS for 60 min and then incubated in 0.3% hydrogen peroxide for 30 min at room temperature. After rinsing in PBS, the sections were incubated in PBS containing 3% horse serum and 0.25% Triton-X for 2h. The sections were then incubated in the primary antibody (1ug/ml) overnight at 4°C, rinsed for 60 min, followed by incubation in biotinylated horse anti-rabbit IgG (Vector Laboratories, Burlingame, CA) diluted 1:200 in PBS for 2 h at room temperature. After additional rinses in PBS for 60 min, the sections were treated with avidin-biotin conjugate (Vectastain ABC kit, Vector Laboratories) and PBS containing 0.04% 3-3'-diaminobenzidine hydrochloride (DAB) reaction and 0.04% nickel ammonium sulfate for 10 min. The sections were then mounted on gelatin coated slides; air dried overnight, dehydrated 2 min each in 70%, 95% and 100% ethyl alcohol followed by 2 min in xylene and then cover slipped with Permount. Second sets of both forebrain and hindbrain sections were utilized to validate the specificity of the TRPV2 antibody by competition with unconjugated control peptide (10ug/ml) that was provided by the supplier.

Double Immunostaining

A third set of free-floating sections from each forebrain were stained for arginine vasopressin (AVP) using a commercially available polyclonal guinea pig anti-AVP (1:1000, Peninsula Laboratories, San Carlos, CA; (Drouyer, et al., 2010)). The sections were incubated overnight in a cocktail of the primary antibodies directed against TRPV2 and AVP. After rinsing, the sections were sequentially incubated in Cy3- conjugated Affinipure Donkey anti-guinea pig IgG (Jackson ImmunoResearch secondary antibody for 4 h followed by Dylight 488-conjugated Affinipure donkey anti-rabbit IgG (Jackson ImmunoResearch, West Grove, PA) for another 4 h, followed by PBS rinsing. The sections were then mounted on gelatin coated slides, air dried overnight and then cover slipped with Vectashield (Vector Laboratories). The final sets of forebrain sections were stained for glial fibrillary acidic protein (GFAP; mouse monoclonal, Sigma Aldrich, St. Louis, MO) and TRPV2. For this, PBS rinsed sections were incubated in a cocktail of antibodies against TRPV2 (1:100) and GFAP (1:1500). After overnight incubation, the sections were incubated in a cocktail of Cy3 conjugated donkey anti-guinea pig IgG and Dylight 488-conjugated Affinipure donkey anti-rabbit IgG (Jackson ImmunoResearch, West Grove, PA) for 4h. The third set of hindbrain free floating sections were stained for Dopamine β- hydroxylase (DBH) using commercially available mouse monoclonal anti dopamine beta hydroxylase (1:1000, MAB308 Millipore, Billerica, MA; (Berglöf, et al., 2009)) and for TRPV2 as described earlier using a Cy3 labeled donkey anti-mouse secondary and a Cy2 labeled donkey anti-rabbit secondary antibody.

Brightfield and Confocal Imaging

TRPV2 positive cells were examined and analyzed using an Olympus IX-2 DSU confocal microscope equipped for brightfield imaging and for epifluorescence with appropriate excitation/emission filter sets. Images were captured using a Q-imaging Retiga-SRV camera. The areas analyzed were identified using Paxinos and Watson (1997) for the forebrain and Paxinos (1999) for the hindbrain. For analysis of TRPV2/AVP double labeling, sections containing the supraoptic nucleus of the hypothalamus (SON) located -0.80 mm to −1.80 mm posterior to bregma were analyzed. For paraventricular nucleus of the hypothalamus (PVN), sections located at −1.40 mm to −2.12 mm posterior to bregma were utilized for analysis. For analysis of DBH/TRPV2 colocalization, sections containing the NTS from −13.175 mm to −14.066 mm posterior to bregma were analyzed. We used Image J software for counting of TRPV2, AVP and DBH labeled cells.

Semiquantitative analysis of TRPV2 distribution

To evaluate the relative densities and distribution patterns of TRPV2 positive neurons, brightfield images of immunostained regions were captured from the different areas of the brain. The relative intensity of TRPV2 was graded throughout the brain according to scale of strong (+++), moderate (++), weak (+) and undetectable (−).

Laser Capture Microdissection of magnocellular AVP neurons

AVP Immunostaining for LCM—Rats (n = 5) were anesthetized with thiobutabarbital (Inactin, Sigma, 100mg/kg ip) and decapitated. Brains were rapidly removed and were snap frozen in cooled isopentane kept on dry ice. Using a cryostat10μm thick serial frozen sections were cut through the hypothalamus at the level of the SON and mounted onto Polyethylene Napthalate (PEN) membrane coated slides (Catalogue# LCM0522- Arcturus Bioscience). Frozen sections were allowed to thaw for 30 sec on the slides. The sections were fixed in ice-cold 100% methanol for 3 min followed by washing in cold DEPC- PBS three times. Blocking was done DEPC- PBS containing 3% horse serum and 0.25% Triton-X for 5 min. This was followed by incubation in guinea pig anti-AVP antibody diluted 1:50

in DEPC- PBS diluent for 3 min and incubation in donkey anti-guinea pig Cy3-labeled secondary antibody diluted 1:50 in DEPC-PBS for 3 min (Carreno, et al., 2011).

Laser Capture Microdissection (LCM) of AVP neurons—An Arcturus Veritas Microdissection instrument, which utilizes the IR capture laser with a UV cutting laser, was used to laser capture AVP labeled neurons. Only neurons that exhibited visible and complete cytoplasmic staining were selected for LCM harvesting. After dissecting individual immunoreactive neurons from surrounding tissue, each cell was captured into an Arcturus Adhesive Cap. After the cells were collected, the cap was immediately transferred to a 0.5ml tube containing 30 μl of ArrayPure Nano-Scale Lysis Solution with 5.0 μ g of proteinase K (prod. no. MPS04050; Epicentre Biotechnol Inc. Madison, WI, USA).

Single-neuron RNA extraction and amplification—Total RNA was isolated from each of 7–10 neurons collected per animal with ArrayPure Nano-Scale RNA Purification Kit reagents (Epicentre Biotechnol Inc.), in accordance with the manufacturer's instructions. Briefly, the cells were individually incubated in Lysis Solution for 15 min at 65–70 °C, and protein was precipitated by addition of 18 μl of MPC Protein Precipitation, followed by vortexing and centrifugation at 10, 000 g for 7 min at 4 °C. Fifty microlitres of isopropanol was added to the supernatant, followed by centrifugation at 10, 000 g for 5 min at 4 °C. Contaminating DNA was removed from preparations: pellets were air-dried for 5 min, suspended in 20 μl of DNase I solution containing 1 μl of RNase- Free DNase I and 40μl of 1X DNase buffer, and incubated for 10 min. After addition of 20 μl each of 2X Nano-Scale Lysis Solution and MPC Protein Precipitation Reagent, the mixtures were vortexed and centrifuged at 10, 000 g for 5 min at 4 °C. After the addition of 50 ul isopropanol, the supernatants were centrifuged at 10,000 g for 5 min at 4 °C to pellet purified RNA. Final rinsing was carried out with 70% ethanol. Resulting pellets were air-dried for 5 min, and resuspended in 5 μl of RNase-Free water supplemented with 1μl of ScriptGuard RNase inhibitor (Epicentre Biotechnol Inc.). All RNA samples were stored at - 80° C. RNA samples were evaluated using a Nanodrop Spectrophotometer (Nanodrop 2000c Spectrophotometer, Thermoscientific). An aliquot of 1–2 μl per cellular RNA sample was amplified with TargetAmp 2-Round Aminoallyl-aRNA Amplification Kit materials (Epicentre Biotechnol Inc.), in accordance with the manufacturer's instructions as previously described (Briski, et al., 2010, Carreno, et al., 2011).

qRT-PCR—Aminoallyl-aRNA (< 50 ng) from laser-micro dissected neurons was reverse-transcribed to cDNA with Sensiscript RT Kit reagents (prod. no.205213; Qiagen Inc., Valencia, CA, USA), in accordance with the manufacturer's instructions. Each RT reaction mixture consisted of 2μl of 10X RT buffer, 2μl of dNTP mix (final concentration: 5 mM), 2μl of oligo-dT primer solution (final concentration: 10 μm), 1 μl of RNase inhibitor (final concentration: 10 U / μl), 1μl of Sensiscript reverse transcriptase solution, and aRNA dissolved in sufficient RNase-free water to yield a total volume of 20 μl. Forward and reverse primers for target genes (Table 1) were obtained from Integrated DNA Technologies (Coralville, Iowa, USA). PCR samples consisted of 2μl of cDNA, 10.3μl of RNase / DNase-free water, 0.2μl of each primer, and 12.5μl of iQ SYBR Green Supermix (prod. no. 170-8880; Bio-Rad). PCR reactions were performed in a Bio-Rad iQTM5 iCycler system, with cyclic parameters: initial denaturation at 95 °C for 3 min, followed by 40 cycles of 1 min each (40 s at 94°C; followed by 30 s at 60 °C, 72° at 40s).The housekeeping gene, GAPDH, was measured for normalization of mRNA expression in each sample. In each real-time RT-PCR analysis, no-template and no-RT controls were performed. Melt curves generated were analyzed to identify nonspecific products and primer-dimers. The data was analyzed by the $2^{-\Delta CT}$ method as described previously (Carreno, et al., 2011).

Results

Characterization of the TRPV2 antibody staining

The specificity of the TRPV2 antibody was first assessed by pre-incubation of the antibody with the control peptide supplied by the manufacturer. Figure 1 shows representative images of TRPV2-postive cell body staining in the SON (Fig. 1A) and PVN (Fig. 1B). The robust TRPV2-ir seen in the SON and PVN were completely abolished by the addition of the control peptide illustrating the specificity of the TRPV2 antibody (Figs. 1C &1D). The control peptide also blocked TRPV2 staining in regions outside the hypothalamus including the cortex (Fig 1E) and the NTS of the hindbrain (Fig 1F). Additional characterization of the antibody was carried out using TRPV2 knockout mouse brains. Figure 2 shows wild-type (WT) and TRPV2 knockout (KO) mice stained for TRPV2 immunoreactivity. Robustly stained TRPV2-ir cells in the SON from WT are shown in Fig 2A. However in the KO there is absence of TRPV2 staining in the SON (Fig. 2B). In the hindbrain, TRPV2 staining seen in the WT was absent in the KO (Fig. 2C & 2D). As reported previously (Park et al., 2011), somatosensory neurons in WT dorsal root ganglia were intensely labeled with TRPV2 antibody, whereas KO ganglia did not show specific staining (Fig 2E & 2F).

Characterization of TRPV2 distribution in the hypothalamus and forebrain regions by single immunohistochemistry

Table 2 shows the relative abundance of the TRPV2 immuno-reactive neurons in the different areas of the forebrain. The densest immunolabeling was observed in the magnocellular SON in both the rostral and caudal aspects (Fig. 1A & 2A) and in magnocellular PVN (Fig. 1B & 2B). TRPV2 immunoreactive processes also were observed in the posterior pituitary (Fig.3C & 3D). Moderate numbers of TRPV2 stained cell bodies were evident in the posterior parvocellular and dorsal horn region of the paraventricular nucleus of the hypothalamus (Fig. 4A). The organum vasculosum of the lamina terminalis (OVLT), located in the ventral lamina terminalis, contained intense staining of neuropil and fibers (Figs. 4B and 4G). TRPV2 positive cells were located in both the lateral and dorsal aspects of the nucleus of the OVLT. In contrast, the median preoptic nucleus (MnPO) contained moderate cell body staining ventral and dorsal to the anterior commissure (Figs. 4C and 4H) while the subfornical organ (SFO), the other circumventricular organ of the lamina terminalis, displayed moderate fiber staining but few TRPV2 positive cells (Fig. 4D). Moderate staining of cell bodies was observed in the arcuate nucleus of the hypothalamus (ARH) (Fig. 4E). Mild TRPV2 staining was present in the medial forebrain bundle (MFB) (Fig. 4F). Mild TRPV2 staining also was observed in cingulate cortex, globus pallidus and hindlimb forelimb (HLFL) somatosensory cortex (Figs. 5A–C). Very little or no immunostaining for TRPV2 was observed in the suprachiasmatic nucleus, ventromedial and dorsomedial hypothalamus, lateral hypothalamic region.

Characterization of TRPV2 distribution in the hindbrain by single immunohistochemistry

The relative abundance of the TRPV2 immunopositive cells in different areas of the hindbrain is shown in Table 3. Dense labeling of cell bodies was evident in the dorsal vagal complex (DVC) and the hypoglossal nucleus (Fig. 6A). A few small immunostained TRPV2 cells were located in the cap region of the area postrema (AP) (Figs.6B & 6C) and dense fiber staining was observed in the Nucleus of the solitary tract (NTS) bordering the area postrema and this region also contained numerous immunoreactive cell bodies (Figs. 6B and 6D). Intense cell body staining was located in the nucleus ambiguous with moderate staining ventral to the nucleus ambiguous in the ventrolateral medulla (VLM) (Figs. 7A and 7B). Few TRPV2 immunoreactive cells were observed in the raphae pallidus nucleus. Figure 8 shows representative TRPV2 staining seen in the C2 adrenaline cells (Fig.8A), pontine nucleus caudal (Fig. 8B), laterotegmental (Fig. 8C) and lateral reticular nucleus (Fig. 8D)

Co-localization of TRPV2 protein with AVP neurons in the SON and PVN and with DBH in the caudal NTS and ventrolateral medulla

Double label immunoflourescence studies revealed that the TRPV2 immunoreactive neurons in the SON co-localized with the AVP neuronal cell bodies in the SON and the magnocellular PVN of the hypothalamus. Confocal images of the AVP/TRPV2 colocalization in the SON and caudal magnocellular PVN are represented in Figure 9. To investigate whether the TRPV2 is expressed in noradrenergic cell groups in the hindbrain, double immunoflourescent studies were carried out for TRPV2 and DBH. We found a mild to moderate level of co-localization of TRPV2 with DBH in the caudal A2 region of the NTS as shown in Figure 10A–C and in the rostral division of the ventrolateral medulla as depicted by representative images in Figure 10D–F. Table 4 shows the TRPV2/AVP counts in the SON and TRPV2/DBH colocalization counts in the NTS. Approximately 74% of the vasopressin immunoreactive cells in the SON were found to be TRPV2 positive. The percentage of DBH positive neurons co-labeled for TRPV2 was approximately 34%.

Double Immunostaining of TRPV2 protein with GFAP positive astrocytes

Double immunostaining of TRPV2 and GFAP showed low to undetectable levels of double labeling in the ventral glia lamina of the SON. GFAP labeled processes were observed distributed among the MNC soma of the SON and very few of these processes stained positively for TRPV2. Figure 11 shows representative confocal images of GFAP (Figure 11A), TRPV2 (Figure 11B), and TRPV2/GFAP double immunostaining in the SON. In the arcuate nucleus (Fig. 12A) and MFB (Fig. 12B), colocalization of TRPV2 and GFAP was also very low to undetectable.

Gene expression analysis

The AVP immunoreactive neurons were identified by a quick immunostaining protocol involving guinea pig polyclonal primary antibody and Cy3 secondary antibody as previously described in our earlier publications (Carreno, et al., 2011, Nedungadi, et al., 2012). The method and area used for microdissection causes minimal damage to the tissue surrounding the neurons.

Figure 13 show the amplification curves for GAPDH (A), TRPV2 (B) and AVP (C) and genes from the samples wells. All the CT values for the genes of interest were in the range from 25–30 and the CT values for the GAPDH were in the lower 20s. ΔCT values were calculated by subtracting the housekeeping (GAPDH) CT value from the gene of interest. The 2-ΔCT values for AVP and TRPV2 mRNA expression are as follows. The $2^{-\Delta CT}$ value for AVP was 0.07144 ± 0.03183 and the $2^{-\Delta CT}$ value for TRPV2 = 0.01511 ± 0.00194. These values correspond to robust mRNA levels of AVP and TRPV2. Lower values in 3–4 decimal places indicate high CT values and correspond to lower mRNA levels. These results indicate that the gene encoding TRPV2 is expressed in AVP neurons in the SON.

Discussion

Our study provides a systematic examination of TRPV2 protein in the rat forebrain and hindbrain focusing on brain regions involved in autonomic regulation and body fluid homeostasis. In the forebrain, there was extensive TRPV2 immunoreactivity in the magnocellular neurons of the SON and PVN and in the OVLT. TRPV2 was colocalized with AVP in both the SON and PVN as demonstrated by double labeling and confocal microscopy. This observation also is supported by data from laser capture microdissection and real time RT-PCR analysis of AVP neurons harvested from the SON which demonstrated expression of TRPV2 mRNA. TRPV2 staining was also present in non-vasopressin neurons in both the PVN and SON indicating its expression in oxytocin

neurons. Our recently published study demonstrates TRPV2 colocalization with oxytocin (Nedungadi, et al., 2012). As reported by Wainwright et.al (2004) in primate brains, we also found beaded TRPV2 fiber staining in addition to staining of the soma in the magnocellular hypothamic areas indicative of dendritic core vesicles containing neurosecretory granules. In rodents, vasopressin and oxytocin magnocellular neurosecretory cells are intrinsically osmosensitive (Mason, 1980, Oliet and Bourque, 1992, Oliet and Bourque, 1993, Renaud and Bourque, 1991). VGL astrocytic processes projecting dorsally showed very low or no co-localization with TRPV2 positive cells in the SON, as well as in the ARH and the MFB respectively. Very few of these astrocytic processes were seen juxtapositioning with TRPV2 labeled cells, suggesting a predominantly neuronal rather than astrocytic localization. While we cannot at this time exclude the possibility that TRPV2 is expressed in astrocytes, our results indicate that if TRPV2 is present in these cells, its expression is very low and that hypothesis may require further investigation.

Dense TRPV2 staining was observed in the OVLT, a circumventricular organ located in the optic recess. Moderate staining of TRPV2 was observed in the MnPO and the SFO which are located on the midline of the anterior wall of the third ventricle in the lamina terminalis. Early functional studies by Andersson et al (1971) and Buggy et al (1979) have shown that the lamina terminalis is involved in osmoregulation. OVLT and other structures located in the lamina terminalis are essential for the normal control of vasopressin release, thirst and salt appetite collectively contributing to maintenance of cardiovascular and body fluid homeostasis (McAllen, et al., 1990, McKinley, et al., 1999, McKinley, et al., 2004). More recent work has demonstrated that the OVLT contains neurons that are osmosensitive (Bourque, et al., 2007). The differences in TRPV2 staining in the SFO and OVLT could be related to their topographically distinct patterns of Fos staining following osmotic stimulation (McKinley, et al., 2004).

We also observed TRPV2 staining in the posterior parvocellular cell group and dorsal cap of the PVN. These regions of the PVN project to the brainstem and spinal cord and are involved in autonomic regulation. Yahamashita et al. (1988) reported that osmotic stimulation of PVN neurons in a brain slice preparation was associated with decreased activity and that PVN neurons display thermosensitivity. However, a more recent report indicates that putative preautonomic neurons in the PVN are depolarized by hypertonic NaCl *in vitro* (Chu, et al., 2010). Our results suggest that TRPV2 could mediate the thermo- or osmosensitivity of these PVN neurons.

Our data on the localization of TRPV2 in the arcuate nucleus of the hypothalamus suggests its possible involvement in food intake and energy homeostasis despite its conspicuous absence in the ventromedial hypothalamus, dorsomedial hypothalamus as well as the lateral hypothalamic area. However, arcuate nucleus exhibit specific neuroendocrine phenotypes (Everitt, et al., 1986).Neurons expressing growth hormone-releasing hormone (GHRH) neurons are predominantly located in the ventrolateral part of the arcuate nucleus, and as we observed a few cells in this region, it is also possible that TRPV2 might play a role in regulating GH release from the pituitary. Interestingly, in contrast to the study on nonhuman primate brain, we did not observe any TRPV2 labeling in the SCN and hence no colocalization with vasopressin in this region. Species variability might account for this difference.

Intense TRPV2 labeling was seen in several areas of the rat hindbrain. We observed abundant TRPV2 immunoreactivity in all aspects of the NTS, the dorsal motor nucleus of the vagus, the hypoglossal nucleus, rostroventrolateral reticular nucleus, caudoventrolateral reticular nucleus the nucleus ambiguous, and the locus coeruleus. Furthermore, we observed that TRPV2 in the NTS and ventrolateral medulla was colocalized with dopamine-beta-

hydroxylase indicating its expression in noradrenergic and adrenergic neurons. In the NTS and the area postrema, there was also dense labeling of fibers throughout each region. The NTS, which receives inputs from primary visceral afferent fibers, is a key relay nucleus in the reflex control of respiratory and autonomic function (Guyenet, 2006, Kalia, 1981). TRPV2 expression in parasympathetic and somatic motor neurons of the rat has been previously described (Lewinter, et al., 2008). The presence of TRPV2 in catecholaminergic neurons in the NTS, ventrolateral medulla, and locus coeruleus suggest that it could participate in the central regulation of neuroendocrine function, sympathetic tone, arousal, and affect (Moreira, et al., 2006, Rinaman, 2007, Rinaman, 2011, Sara, 2009). Lesions of area postrema have been implicated in impaired osmoregulation (Curtis, et al., 1999). Our observation of presence of TRPV2 in the area postrema could possibly imply its possible osmoregulatory component in this region.

TRPV channels have been shown to form homomultimers or heteromers with other members of the same subfamily (Liapi and Wood, 2005, Rutter, et al., 2005). Co-expression of TRPV2 with other TRPV channels in the same cells could result in the formation of heteromeric channels. In the TRPV subfamily, TRPV4 and TRPV1 are other members that are also responsive to osmotic stimulation. Hence it can be speculated that heteromeric assembly of two distinct TRPV channels could result in a gain of function or influence the gating properties of the channel. Capsaicin-sensitive TRPV1 is considered a molecular integrator of physical and chemical pain stimuli (Tominaga and Caterina, 2004). TRPV1 knock-out animals (Caterina, et al., 2000, Caterina, et al., 1997, Davis, et al., 2000) failed to develop thermal hyperalgesia establishing the role of TRPV1 as an important regulator of pain signal transduction mechanisms. It has been suggested that an N -terminal variant of TRPV1 is involved in thermal and osmosensory transduction in the mouse supraoptic neurons (Sharif Naeini, et al., 2006). The osmosensory signal transduction cascade is significantly diminished in TRPV1 KO mice and these mice have significantly attenuated water intake to systemic hypertonicity compared to wild type controls (Ciura and Bourque, 2006). However, TRPV1 KO mice have normal responses to systemic hypernatremia (Taylor, et al., 2008). A possible role for TRPV4 in osmotic regulation has also been suggested. When challenged with systemic hypertonic saline, TRPV4 KO mice exhibited impaired regulatory responses that include decreased water intake and vasopressin release resulting in elevated plasma osmolality (Liedtke and Friedman, 2003). These mice also demonstrated an attenuation of c-Fos expression in the OVLT suggested an impaired activation of this region in response to a hypertonic stress. Previous studies from our lab have identified that in conditions of inappropriate vasopressin release, there is increased expression of TRPV4 protein in the SON of bile duct ligated rats compared to the shams (Carreno, et al., 2009). TRPV2 may contribute to thermo- and osmosensitivity of magnocellular neurosecretory neurons and the OVLT alone or by interacting with other TRPV channels (Sudbury, et al., 2010, Wainwright, et al., 2004).

We have provided evidence for the neuroanatomical distribution of both the mRNA and protein TRPV2 in the rat and its extensive immunolocalization in the magnocellular paraventricular and supraoptic nucleus in the forebrain and colocalization of TRPV2 with vasopressin in these regions. Also, in the hindbrain, extensive TRPV2 expression was seen in the nucleus of the solitary tract, the rostroventrolateral nucleus, the caudoventrolateral nucleus and the hypoglossal nucleus. Our data strongly suggest the possible direct involvement of TRPV2 in mediating osmotic balance, autonomic functions, somatosensory functions, food intake and cardiovascular regulation. This cation channel might also be indirectly involved in mediating other responses apart from its direct actions. In pancreatic β-cells, TRPV2 trafficking and function is modulated by insulin and insulin-like growth factors (Hisanaga, et al., 2009) while cannabinoids and peptides can activate TRPV channels in the nervous system (Chakfe and Bourque, 2001, Flores, et al., 2004, Jeske, et al., 2006).

Our results provide evidence for a new substrate for this type of modulation in each of these regions. TRPV2 knockout mice have compromised immune function and this channel has been shown to play an essential role in macrophage phagocytosis (Link, et al., 2010). Based on our results TRPV2 may play an important role in many CNS networks. Experimental strategies in which TRPV2 is selectively inhibited or knocked down in neurons expressed in different brain areas may shed light on the functional role of this channel in the nervous system.

Acknowledgments

Authors acknowledge the technical assistance of Joel T. Little and Xiangle Sun of the UNTHSC laser capture microdissection core facility. We thank Una Park for generation of the TRPV2 knockout mice and critical reading of the manuscript. This study was supported by National Heart, Lung, and Blood Institute Grant R01 HL062579 (to J.T. Cunningham).

Literature Cited

1. Andersson B. Thirst--and brain control of water balance. Am Sci. 1971; 59:408–415. [PubMed: 4326101]
2. Beech DJ, Muraki K, Flemming R. Non-selective cationic channels of smooth muscle and the mammalian homologues of Drosophila TRP. J Physiol. 2004; 559:685–706. [PubMed: 15272031]
3. Berglöf E, Small BJ, Bickford PC, Strömberg I. Beneficial effects of antioxidant-enriched diet for tyrosine hydroxylase-positive neurons in ventral mesencephalic tissue in oculo grafts. The Journal of Comparative Neurology. 2009; 515:72–82. [PubMed: 19399894]
4. Bourque CW, Ciura S, Trudel E, Stachniak TJ, Sharif-Naeini R. Neurophysiological characterization of mammalian osmosensitive neurones. Exp Physiol. 2007; 92:499–505. [PubMed: 17350993]
5. Briski KP, Nedungadi TP, Koshy Cherian A. Effects of hypoglycaemia on neurotransmitter and hormone receptor gene expression in laser-dissected arcuate neuropeptide Y/agouti-related peptide neurones. J Neuroendocrinol. 2010; 22:599–607. [PubMed: 20298458]
6. Buggy J, Hoffman WE, Phillips MI, Fisher AE, Johnson AK. Osmosensitivity of rat third ventricle and interactions with angiotensin. Am J Physiol. 1979; 236:R75–R82. [PubMed: 434190]
7. Carreno FR, Ji LL, Cunningham JT. Altered central TRPV4 expression and lipid raft association related to inappropriate vasopressin secretion in cirrhotic rats. Am J Physiol Regul Integr Comp Physiol. 2009; 296:R454–R466. [PubMed: 19091909]
8. Carreno FR, Walch JD, Dutta M, Nedungadi TP, Cunningham JT. BDNF-TrkB Pathway Mediates NMDA receptor NR2B Subunit Phosphorylation in the Supraoptic Nuclei Following Progressive Dehydration. J Neuroendocrinol. 2011
9. Caterina MJ, Leffler A, Malmberg AB, Martin WJ, Trafton J, Petersen-Zeitz KR, Koltzenburg M, Basbaum AI, Julius D. Impaired nociception and pain sensation in mice lacking the capsaicin receptor. Science. 2000; 288:306–313. [PubMed: 10764638]
10. Caterina MJ, Rosen TA, Tominaga M, Brake AJ, Julius D. A capsaicin-receptor homologue with a high threshold for noxious heat. Nature. 1999; 398:436–441. [PubMed: 10201375]
11. Caterina MJ, Schumacher MA, Tominaga M, Rosen TA, Levine JD, Julius D. The capsaicin receptor: a heat-activated ion channel in the pain pathway. Nature. 1997; 389:816–824. [PubMed: 9349813]
12. Chakfe Y, Bourque CW. Peptidergic excitation of supraoptic nucleus neurons: involvement of stretch-inactivated cation channels. Exp Neurol. 2001; 171:210–218. [PubMed: 11573973]
13. Christensen AP, Corey DP. TRP channels in mechanosensation: direct or indirect activation? Nat Rev Neurosci. 2007; 8:510–521. [PubMed: 17585304]
14. Chu CP, Kannan H, Qiu DL. Effect of hypertonic saline on rat hypothalamic paraventricular nucleus parvocellular neurons in vitro. Neurosci Lett. 2010; 482:142–145. [PubMed: 20637834]

15. Ciura S, Bourque CW. Transient receptor potential vanilloid 1 is required for intrinsic osmoreception in organum vasculosum lamina terminalis neurons and for normal thirst responses to systemic hyperosmolality. J Neurosci. 2006; 26:9069–9075. [PubMed: 16943565]

16. Colbert HA, Smith TL, Bargmann CI. OSM-9, a novel protein with structural similarity to channels, is required for olfaction, mechanosensation, and olfactory adaptation in Caenorhabditis elegans. J Neurosci. 1997; 17:8259–8269. [PubMed: 9334401]

17. Corey DP. New TRP channels in hearing and mechanosensation. Neuron. 2003; 39:585–588. [PubMed: 12925273]

18. Curtis KS, Huang W, Sved AF, Verbalis JG, Stricker EM. Impaired osmoregulatory responses in rats with area postrema lesions. Am J Physiol. 1999; 277:R209–R219. [PubMed: 10409275]

19. Davis JB, Gray J, Gunthorpe MJ, Hatcher JP, Davey PT, Overend P, Harries MH, Latcham J, Clapham C, Atkinson K, Hughes SA, Rance K, Grau E, Harper AJ, Pugh PL, Rogers DC, Bingham S, Randall A, Sheardown SA. Vanilloid receptor-1 is essential for inflammatory thermal hyperalgesia. Nature. 2000; 405:183–187. [PubMed: 10821274]

20. Drouyer E, LeSauter J, Hernandez AL, Silver R. Specializations of gastrin-releasing peptide cells of the mouse suprachiasmatic nucleus. The Journal of Comparative Neurology. 2010; 518:1249–1263. [PubMed: 20151358]

21. Everitt BJ, Meister B, Hokfelt T, Melander T, Terenius L, Rokaeus A, Theodorsson-Norheim E, Dockray G, Edwardson J, Cuello C, et al. The hypothalamic arcuate nucleus-median eminence complex: immunohistochemistry of transmitters, peptides and DARPP-32 with special reference to coexistence in dopamine neurons. Brain Res. 1986; 396:97–155. [PubMed: 2874874]

22. Flores CM, Price TJ, Patwardhan A, Akopian AN, Hargreaves KM. Modulation of trigeminal sensory neuron activity by the dual cannabinoid-vanilloid agonists anandamide, N-arachidonoyl-dopamine and arachidonyl-2-chloroethylamide. British Journal of Pharmacology. 2004; 141:1118–1130. [PubMed: 15006899]

23. Guler AD, Lee H, Iida T, Shimizu I, Tominaga M, Caterina M. Heat-evoked activation of the ion channel, TRPV4. J Neurosci. 2002; 22:6408–6414. [PubMed: 12151520]

24. Guyenet PG. The sympathetic control of blood pressure. Nat Rev Neurosci. 2006; 7:335–346. [PubMed: 16760914]

25. Hatton GI. Glial-neuronal interactions in the mammalian brain. Advances in Physiology Education. 2002; 26:225–237. [PubMed: 12443995]

26. Hisanaga E, Nagasawa M, Ueki K, Kulkarni RN, Mori M, Kojima I. Regulation of calcium-permeable TRPV2 channel by insulin in pancreatic beta-cells. Diabetes. 2009; 58:174–184. [PubMed: 18984736]

27. Hussy N, Deleuze C, Bres V, Moos FC. New role of taurine as an osmomediator between glial cells and neurons in the rat supraoptic nucleus. Advances in Experimental Medicine & Biology. 2000; 483:227–237. [PubMed: 11787602]

28. Ichikawa H, Sugimoto T. VR1-immunoreactive primary sensory neurons in the rat trigeminal ganglion. Brain Res. 2001; 890:184–188. [PubMed: 11164782]

29. Jeske NA, Patwardhan AM, Gamper N, Price TJ, Akopian AN, Hargreaves KM. Cannabinoid WIN 55,212-2 regulates TRPV1 phosphorylation in sensory neurons. J Biol Chem. 2006; 281:32879–32890. [PubMed: 16954222]

30. Kalia M. Brain stem localization of vagal preganglionic neurons. J Auton Nerv Syst. 1981; 3:451–481. [PubMed: 7276442]

31. Kanzaki M, Zhang YQ, Mashima H, Li L, Shibata H, Kojima I. Translocation of a calcium-permeable cation channel induced by insulin-like growth factor-I. Nat Cell Biol. 1999; 1:165–170. [PubMed: 10559903]

32. Knot HJ, Nelson MT. Regulation of membrane potential and diameter by voltage-dependent K+ channels in rabbit myogenic cerebral arteries. Am J Physiol. 1995; 269:H348–H355. [PubMed: 7631867]

33. Lewinter RD, Scherrer G, Basbaum AI. Dense transient receptor potential cation channel, vanilloid family, type 2 (TRPV2) immunoreactivity defines a subset of motoneurons in the dorsal lateral nucleus of the spinal cord, the nucleus ambiguus and the trigeminal motor nucleus in rat. Neuroscience. 2008; 151:164–173. [PubMed: 18063314]

34. Lewinter RD, Skinner K, Julius D, Basbaum AI. Immunoreactive TRPV-2 (VRL-1), a capsaicin receptor homolog, in the spinal cord of the rat. J Comp Neurol. 2004; 470:400–408. [PubMed: 14961565]
35. Liapi A, Wood JN. Extensive co-localization and heteromultimer formation of the vanilloid receptor-like protein TRPV2 and the capsaicin receptor TRPV1 in the adult rat cerebral cortex. Eur J Neurosci. 2005; 22:825–834. [PubMed: 16115206]
36. Liedtke W. Transient receptor potential vanilloid channels functioning in transduction of osmotic stimuli. J Endocrinol. 2006; 191:515–523. [PubMed: 17170210]
37. Liedtke W, Choe Y, Marti-Renom MA, Bell AM, Denis CS, Sali A, Hudspeth AJ, Friedman JM, Heller S. Vanilloid receptor-related osmotically activated channel (VR-OAC), a candidate vertebrate osmoreceptor. Cell. 2000; 103:525–535. [PubMed: 11081638]
38. Liedtke W, Friedman JM. Abnormal osmotic regulation in trpv4−/− mice. Proc Natl Acad Sci U S A. 2003; 100:13698–13703. [PubMed: 14581612]
39. Lin SY, Corey DP. TRP channels in mechanosensation. Curr Opin Neurobiol. 2005; 15:350–357. [PubMed: 15922584]
40. Link TM, Park U, Vonakis BM, Raben DM, Soloski MJ, Caterina MJ. TRPV2 has a pivotal role in macrophage particle binding and phagocytosis. Nat Immunol. 2010; 11:232–239. [PubMed: 20118928]
41. Mason WT. Supraoptic neurones of rat hypothalamus are osmosensitive. Nature. 1980; 287:154–157. [PubMed: 7432448]
42. McAllen RM, Pennington GL, McKinley MJ. Osmoresponsive units in sheep median preoptic nucleus. Am J Physiol. 1990; 259:R593–R600. [PubMed: 2396717]
43. McKinley MJ, Gerstberger R, Mathai ML, Oldfield BJ, Schmid H. The lamina terminalis and its role in fluid and electrolyte homeostasis. J Clin Neurosci. 1999; 6:289–301. [PubMed: 10835180]
44. McKinley MJ, Mathai ML, McAllen RM, McClear RC, Miselis RR, Pennington GL, Vivas L, Wade JD, Oldfield BJ. Vasopressin secretion: osmotic and hormonal regulation by the lamina terminalis. J Neuroendocrinol. 2004; 16:340–347. [PubMed: 15089972]
45. Monet M, Gkika D, Lehen'kyi V, Pourtier A, Vanden Abeele F, Bidaux G, Juvin V, Rassendren F, Humez S, Prevarsakaya N. Lysophospholipids stimulate prostate cancer cell migration via TRPV2 channel activation. Biochim Biophys Acta. 2009; 1793:528–539. [PubMed: 19321128]
46. Moran MM, McAlexander MA, Bíró T, Szallasi A. Transient receptor potential channels as therapeutic targets. Nat Rev Drug Discov. 2011; 10:601–620. [PubMed: 21804597]
47. Moreira TS, Takakura AC, Colombari E, Guyenet PG. Central chemoreceptors and sympathetic vasomotor outflow. J Physiol. 2006; 577:369–386. [PubMed: 16901945]
48. Muraki K, Iwata Y, Katanosaka Y, Ito T, Ohya S, Shigekawa M, Imaizumi Y. TRPV2 is a component of osmotically sensitive cation channels in murine aortic myocytes. Circ Res. 2003; 93:829–838. [PubMed: 14512441]
49. Nagasawa M, Nakagawa Y, Tanaka S, Kojima I. Chemotactic peptide fMetLeuPhe induces translocation of the TRPV2 channel in macrophages. J Cell Physiol. 2007; 210:692–702. [PubMed: 17154364]
50. Nedungadi TP, Carreno FR, Walch JD, Bathina CS, Cunningham JT. Region-specific changes in transient receptor potential vanilloid channel expression in the vasopressin magnocellular system in hepatic cirrhosis-induced hyponatraemia. J Neuroendocrinol. 2012; 24:642–652. [PubMed: 22188460]
51. O'Neil RG, Heller S. The mechanosensitive nature of TRPV channels. Pflugers Arch. 2005; 451:193–203. [PubMed: 15909178]
52. Oliet SH, Bourque CW. Properties of supraoptic magnocellular neurones isolated from the adult rat. J Physiol. 1992; 455:291–306. [PubMed: 1362442]
53. Oliet SH, Bourque CW. Mechanosensitive channels transduce osmosensitivity in supraoptic neurons. Nature. 1993; 364:341–343. [PubMed: 7687327]
54. Park U, Vastani N, Guan Y, Raja SN, Koltzenburg M, Caterina MJ. TRP vanilloid 2 knock-out mice are susceptible to perinatal lethality but display normal thermal and mechanical nociception. J Neurosci. 2011; 31:11425–11436. [PubMed: 21832173]

55. Penna A, Juvin V, Chemin J, Compan V, Monet M, Rassendren FA. PI3-kinase promotes TRPV2 activity independently of channel translocation to the plasma membrane. Cell Calcium. 2006; 39:495–507. [PubMed: 16533525]
56. Renaud LP, Bourque CW. Neurophysiology and neuropharmacology of hypothalamic magnocellular neurons secreting vasopressin and oxytocin. Prog Neurobiol. 1991; 36:131–169. [PubMed: 1998074]
57. Rinaman L. Visceral sensory inputs to the endocrine hypothalamus. Front Neuroendocrinol. 2007; 28:50–60. [PubMed: 17391741]
58. Rinaman L. Hindbrain noradrenergic A2 neurons: diverse roles in autonomic, endocrine, cognitive, and behavioral functions. Am J Physiol Regul Integr Comp Physiol. 2011; 300:R222–R235. [PubMed: 20962208]
59. Rutter AR, Ma QP, Leveridge M, Bonnert TP. Heteromerization and colocalization of TrpV1 and TrpV2 in mammalian cell lines and rat dorsal root ganglia. Neuroreport. 2005; 16:1735–1739. [PubMed: 16237318]
60. Sara SJ. The locus coeruleus and noradrenergic modulation of cognition. Nat Rev Neurosci. 2009; 10:211–223. [PubMed: 19190638]
61. Scotland RS, Chauhan S, Davis C, De Felipe C, Hunt S, Kabir J, Kotsonis P, Oh U, Ahluwalia A. Vanilloid receptor TRPV1, sensory C-fibers, and vascular autoregulation: a novel mechanism involved in myogenic constriction. Circ Res. 2004; 95:1027–1034. [PubMed: 15499026]
62. Sharif-Naeini R, Ciura S, Zhang Z, Bourque CW. Contribution of TRPV channels to osmosensory transduction, thirst, and vasopressin release. Kidney Int. 2008; 73:811–815. [PubMed: 18200003]
63. Sharif Naeini R, Witty MF, Seguela P, Bourque CW. An N-terminal variant of Trpv1 channel is required for osmosensory transduction. Nat Neurosci. 2006; 9:93–98. [PubMed: 16327782]
64. Shibasaki K, Murayama N, Ono K, Ishizaki Y, Tominaga M. TRPV2 enhances axon outgrowth through its activation by membrane stretch in developing sensory and motor neurons. J Neurosci. 2010; 30:4601–4612. [PubMed: 20357111]
65. Sudbury JR, Ciura S, Sharif-Naeini R, Bourque CW. Osmotic and thermal control of magnocellular neurosecretory neurons--role of an N-terminal variant of trpv1. Eur J Neurosci. 2010; 32:2022–2030. [PubMed: 21143657]
66. Szallasi A, Blumberg PM. Vanilloid (Capsaicin) receptors and mechanisms. Pharmacol Rev. 1999; 51:159–212. [PubMed: 10353985]
67. Taylor AC, McCarthy JJ, Stocker SD. Mice lacking the transient receptor vanilloid potential 1 channel display normal thirst responses and central Fos activation to hypernatremia. Am J Physiol Regul Integr Comp Physiol. 2008; 294:R1285–R1293. [PubMed: 18272658]
68. Theodosis DT, Piet R, Poulain DA, Oliet SH. Neuronal, glial and synaptic remodeling in the adult hypothalamus: functional consequences and role of cell surface and extracellular matrix adhesion molecules. Neurochem Int. 2004; 45:491–501. [PubMed: 15186915]
69. Tominaga M, Caterina MJ. Thermosensation and pain. J Neurobiol. 2004; 61:3–12. [PubMed: 15362149]
70. Venkatachalam K, Montell C. TRP channels. Annual Review of Biochemistry. 2007; 76:387–417.
71. Wainwright A, Rutter AR, Seabrook GR, Reilly K, Oliver KR. Discrete expression of TRPV2 within the hypothalamo-neurohypophysial system: Implications for regulatory activity within the hypothalamic-pituitary-adrenal axis. J Comp Neurol. 2004; 474:24–42. [PubMed: 15156577]
72. Watson RE, Wiegland SJ, Clough RW, Hoffman GE. Use of cryoprotectant to maintain long-term peptide immunoreactivity and tissue morphology. Peptides (New York, N.Y.: 1980). 1986; 7:155–159.
73. Welsh DG, Morielli AD, Nelson MT, Brayden JE. Transient receptor potential channels regulate myogenic tone of resistance arteries. Circ Res. 2002; 90:248–250. [PubMed: 11861411]
74. Yamashiro K, Sasano T, Tojo K, Namekata I, Kurokawa J, Sawada N, Suganami T, Kamei Y, Tanaka H, Tajima N, Utsunomiya K, Ogawa Y, Furukawa T. Role of transient receptor potential vanilloid 2 in LPS-induced cytokine production in macrophages. Biochem Biophys Res Commun. 2010; 398:284–289. [PubMed: 20599720]

75. Yamashita H, Inenaga K, Dyball RE. Thermal, osmotic and chemical modulation of neural activity in the paraventricular nucleus: in vitro studies. Brain Res Bull. 1988; 20:825–829. [PubMed: 3409058]

Highlights

- TRPV2 expressed in rat brain regions involved in fluid homeostasis, food intake and autonomic regulation.
- Densest TRPV2 labeling in magnocellular SON and PVN.
- TRPV2 colocalizes with vasopressin in the forebrain and with DBH in the hindbrain.
- Presence of TRPV2 mRNA in vasopressin neurons as detected by LCM and qRT-PCR.

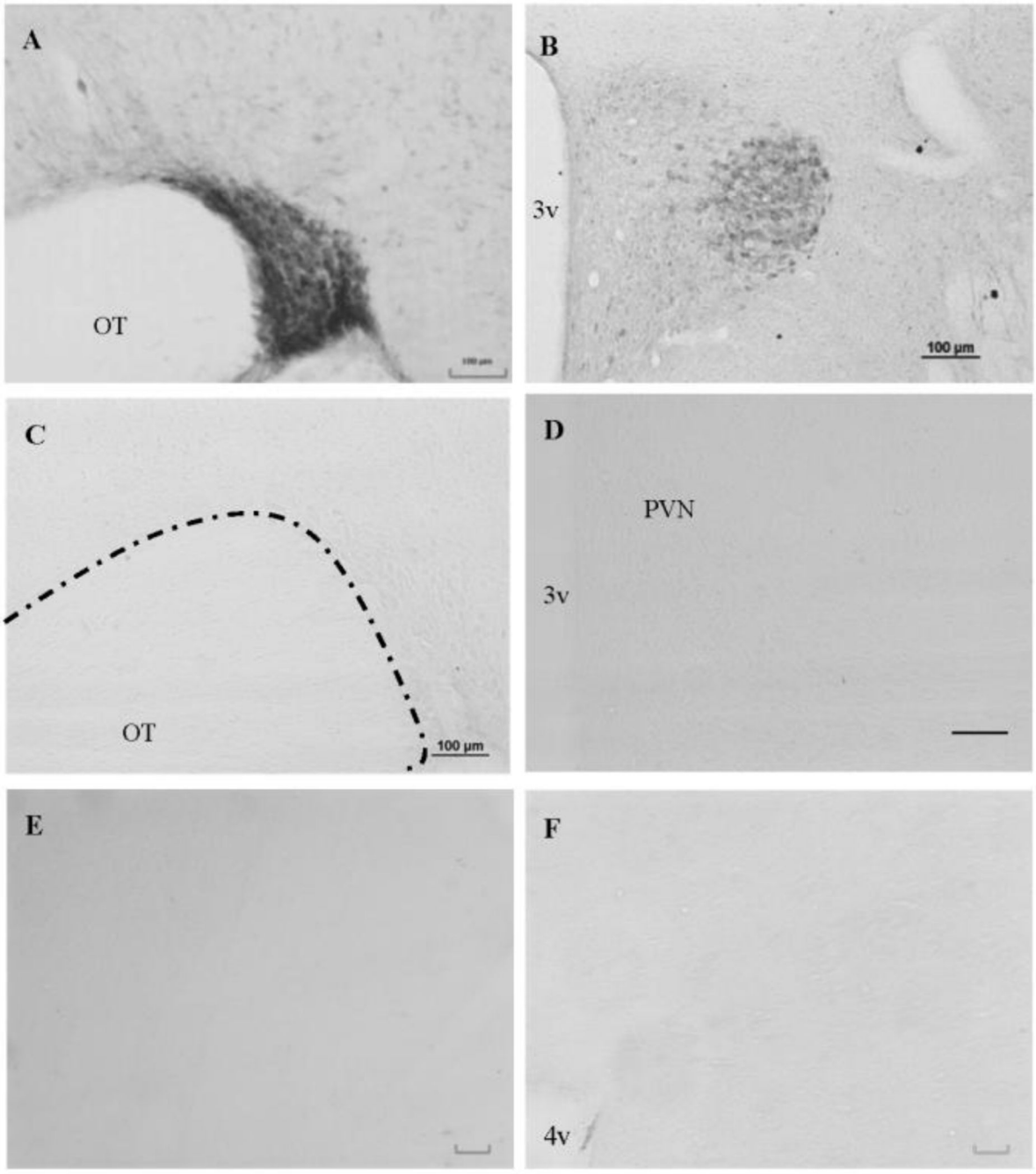

Figure 1.

Demonstration of the specificity of the TRPV2 antibody in the hypothalamic magnocellular areas. Brightfield images of specific staining seen in the SON (A) and the PVN (B) is completely abolished by addition of the pre-absorption peptides. Adding 10X excess pre-absorption peptide eliminated TRPV2 immunostaining in the SON (C), PVN (D), cortex (E) and NTS (F). The third ventricle is represented as 3v and the optic tract is represented as OT. The fourth ventricle is represented as 4v. Scale bars= 100 µm in all the images.

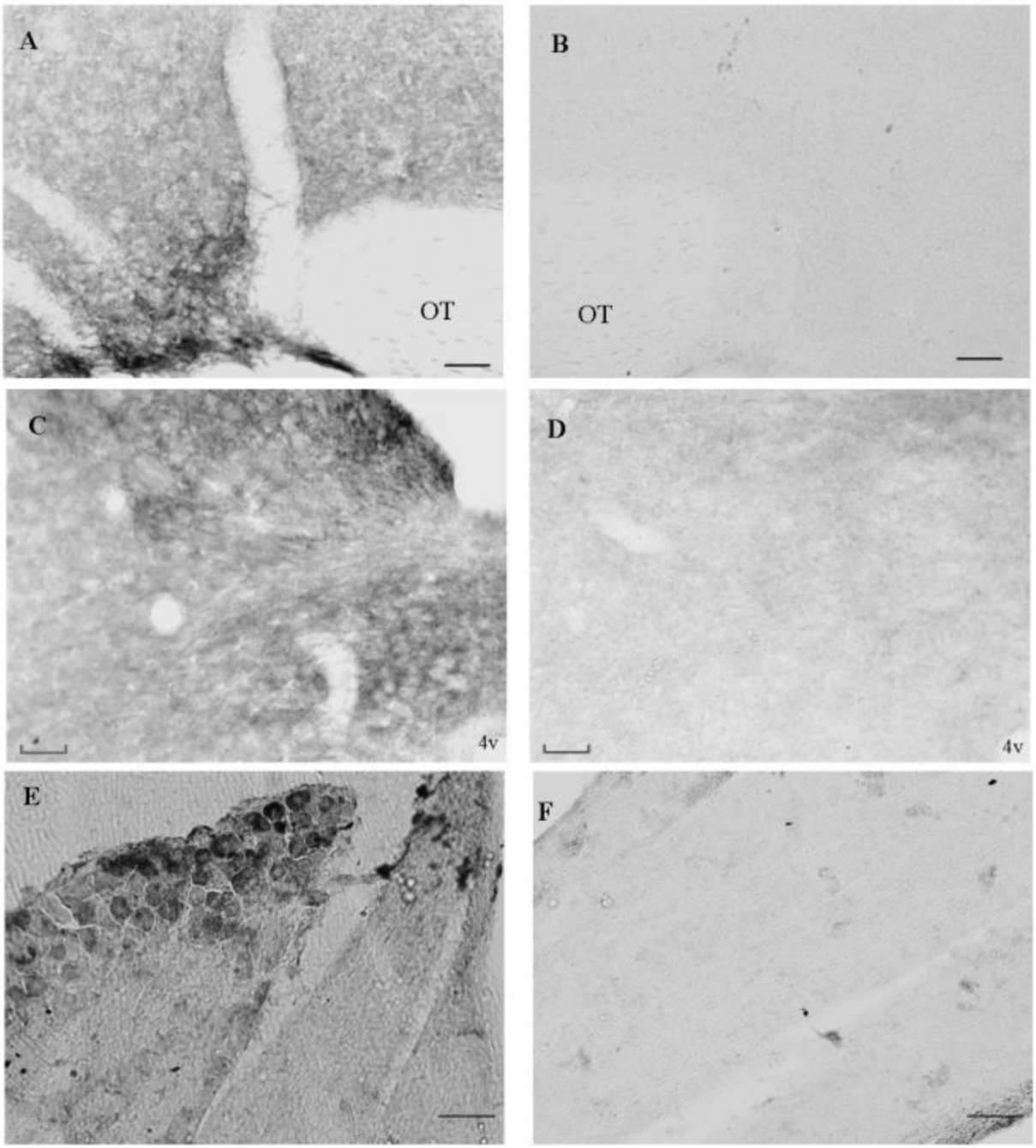

Figure 2.
Antibody specificity tested using TRPV2 KO and WT mouse brain and dorsal root ganglionic tissue using brightfield imaging. Specific staining seen in the SON of WT (A) is completely absent in the SON of the KO mice (B). Similar staining patterns are shown in the NTS of WT (C) and KO (D). As a positive control, presence vs absence of TRPV2 staining in the DRG of WT (E) and KO (F) respectively. Scale bar=100 μm in all the images

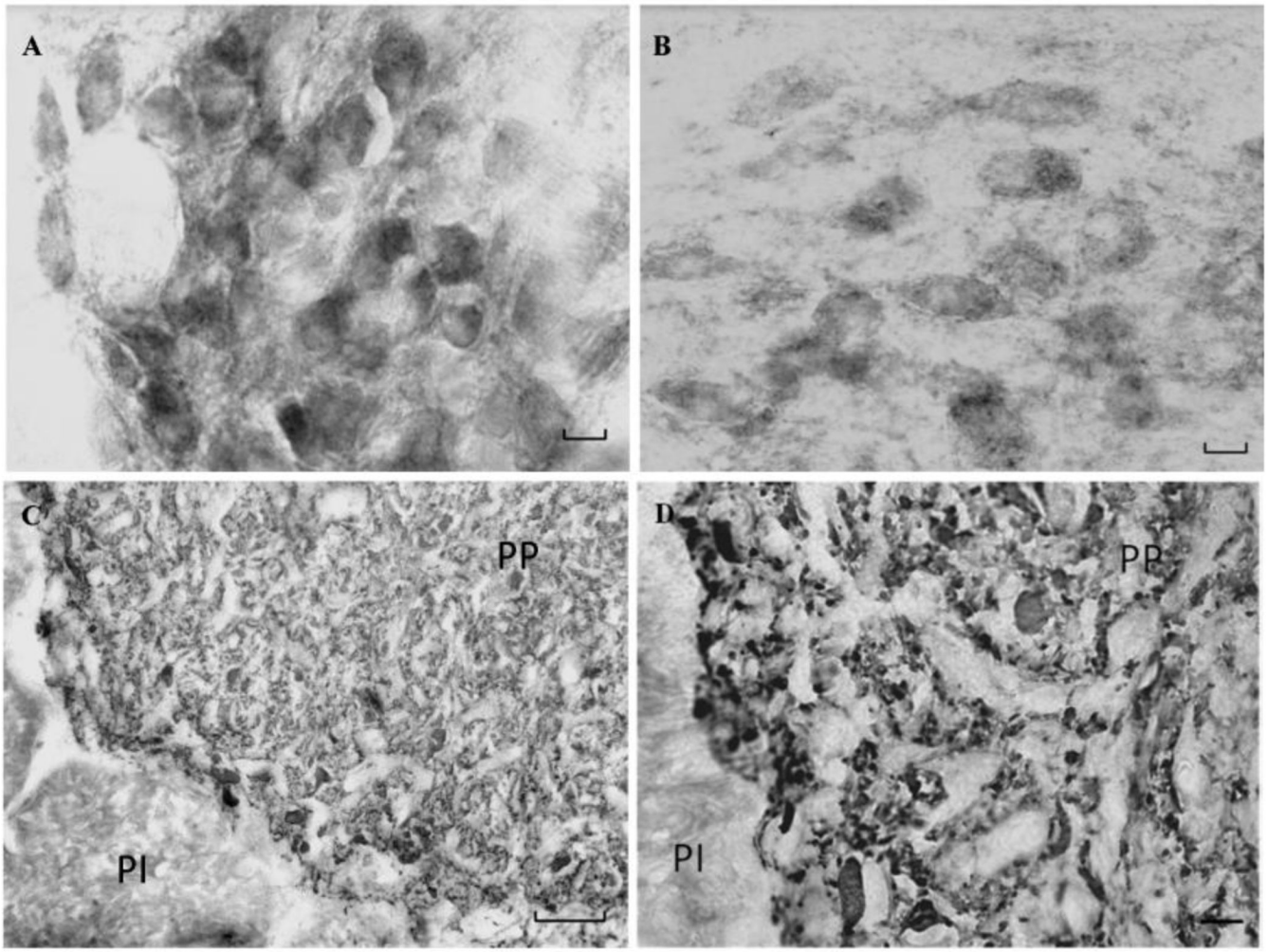

Figure 3.

Brightfield microscopic images of TRPV2 in SON (A), PVN (B), and posterior pituitary (C & D). High magnification images of the SON (A) and the PVN (B) shows intense cell body staining of TRPV2 in these areas. A low magnification image of the pituitary (C) shows TRPV2 immunoreactive process in the posterior pituitary (PP) and less immunostaining in the pars intermedia (PI). High magnification images (D) depict the dense immunostaining in the posterior pituitary. Scale bar= 100 μm in C; 10 μm in A, B and D.

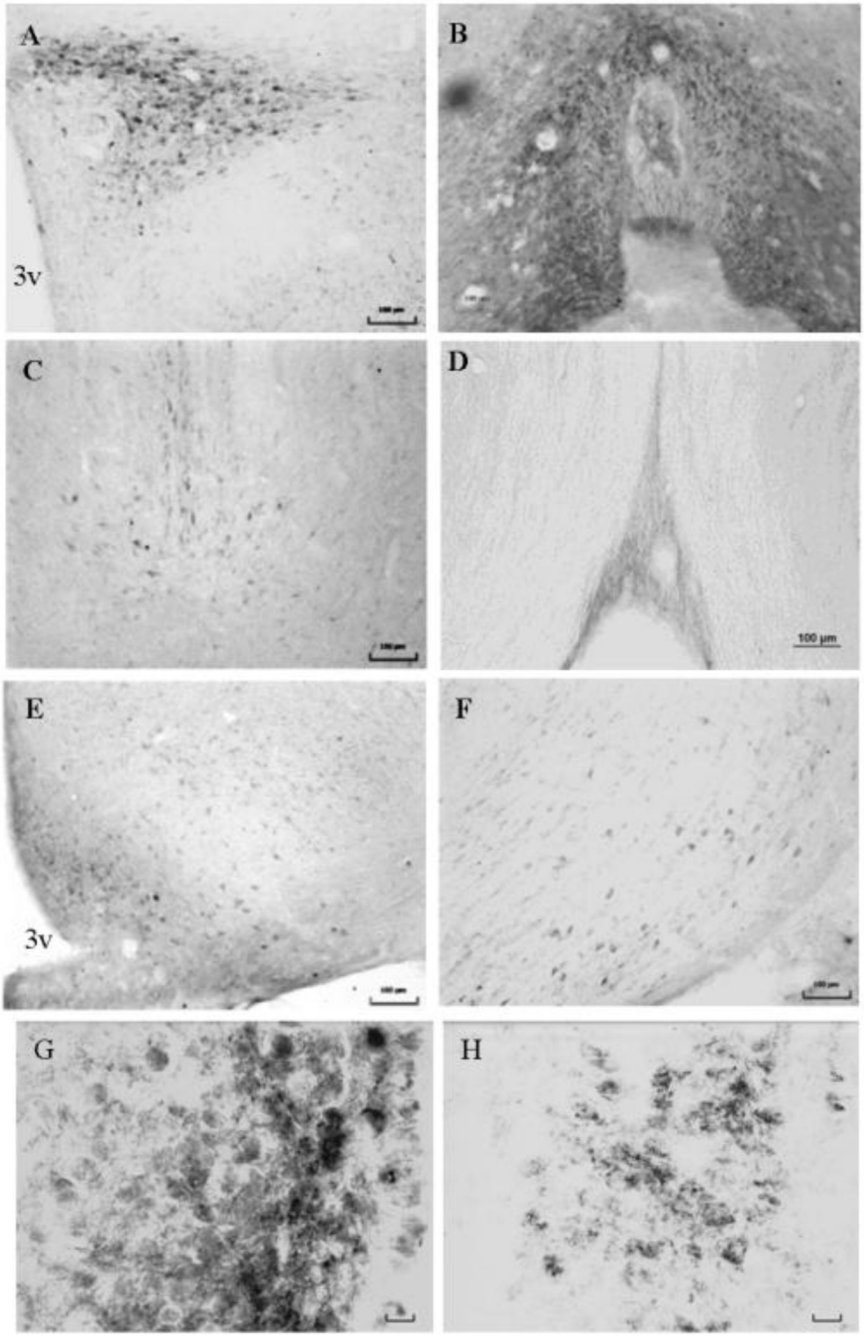

Figure 4.

Expression of TRPV2 in the posterior parvocellular and the dorsal horn of the PVN (A), OVLT (B), MnPO (C), SFO (D), ARH (E) and MFB (F) and high magnification images of intense TRPV2 DAB immunoreactivity in the OVLT (G) and moderate TRPV2 staining in the MnPO (H) 3v represents the third ventricle. Scale bar = 100 µm for images A-F and 10 µm for images G and H.

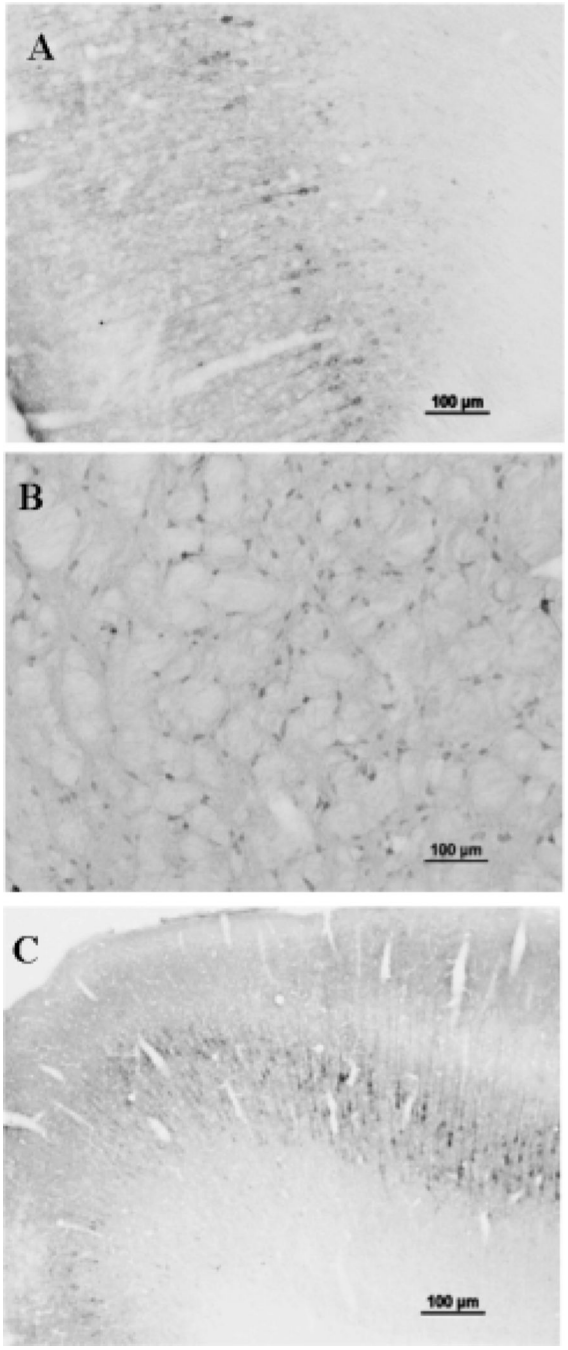

Figure 5.
Images of mild TRPV2 staining in the cingulate cortex (A), globus pallidus (B) and the Hind limb-Forelimb (HLFL) cortex (C). Scale bar=100 µm in all the images.

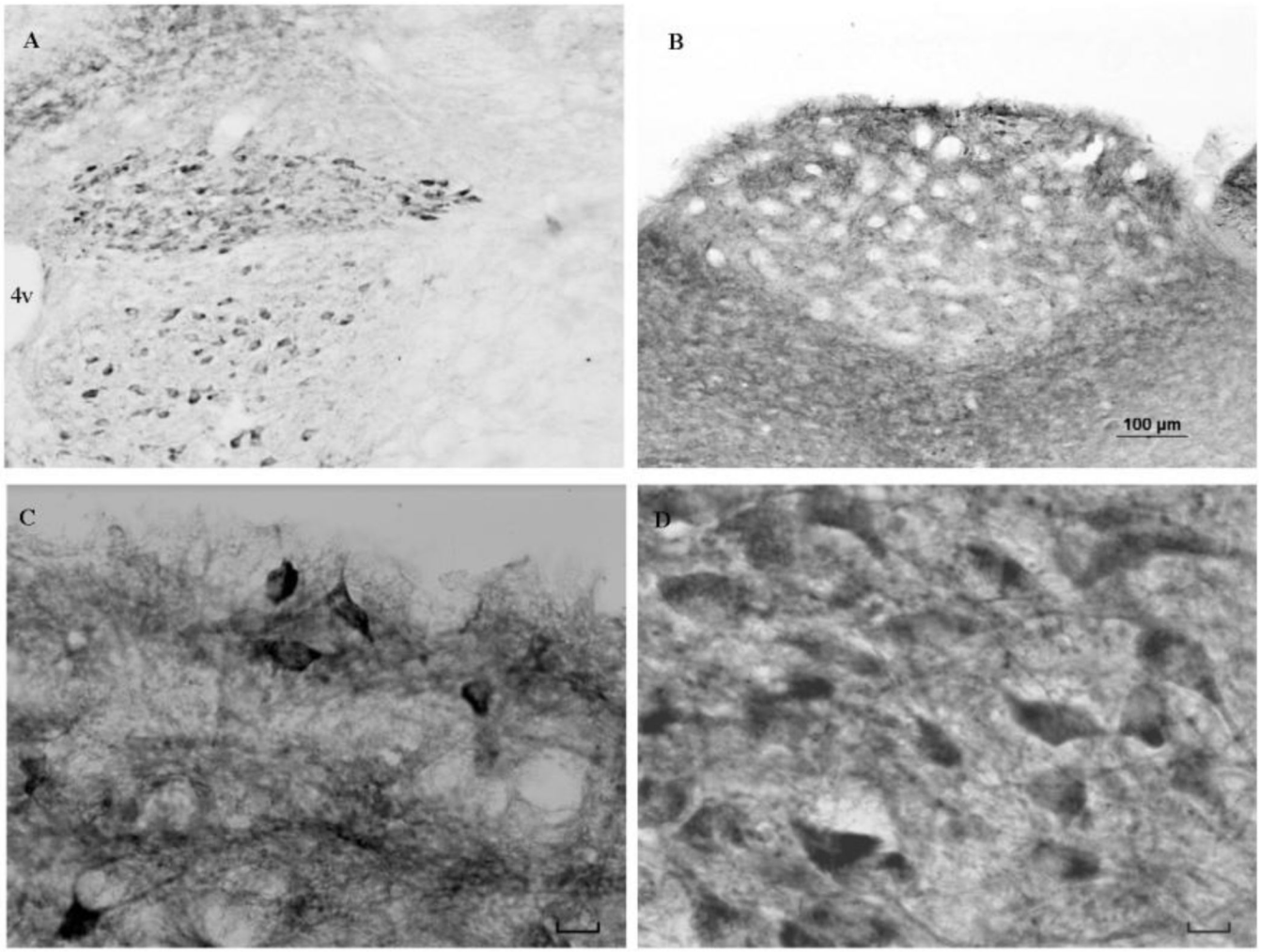

Figure 6.
Expression of TRPV2 in the DVC and hypoglossal nucleus (A) showing dense immunoreactive cell bodies. Dense immunoreactive fiber labeling and small cells expressing TRPV2 located in the dorsal cap of the AP (B). High magnification images of TRPV2 positive cells in the dorsal cap of the AP (C) and in the NTS (D). 4v represents the fourth ventricle. Scale bar = 100μm in A and B. Scale bar = 10 μm for C and D.

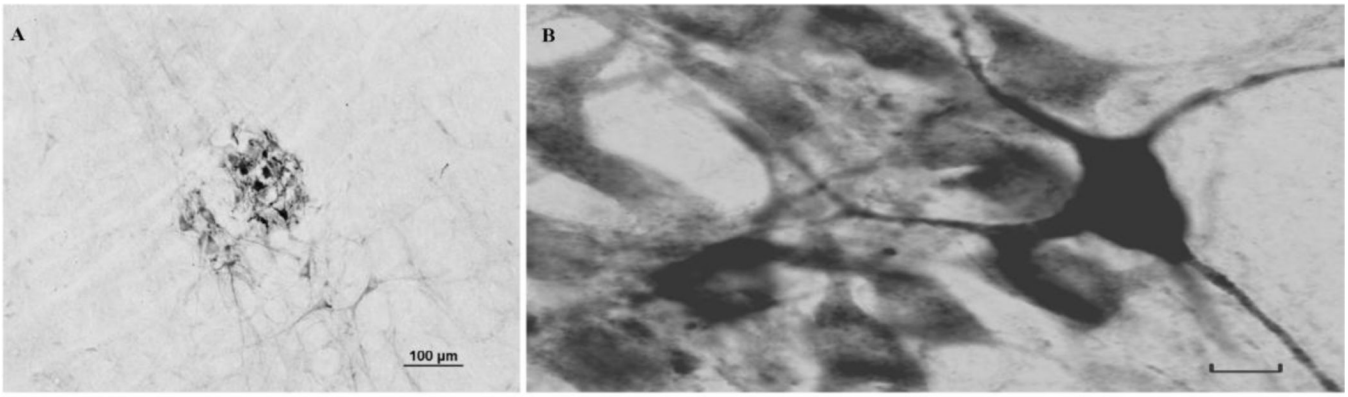

Figure 7.
TRPV2 immunostaining in the nucleus ambiguous and the rostral division of the VLM. Scale bar = 100µm in A. Scale bar = 10 µm for B.

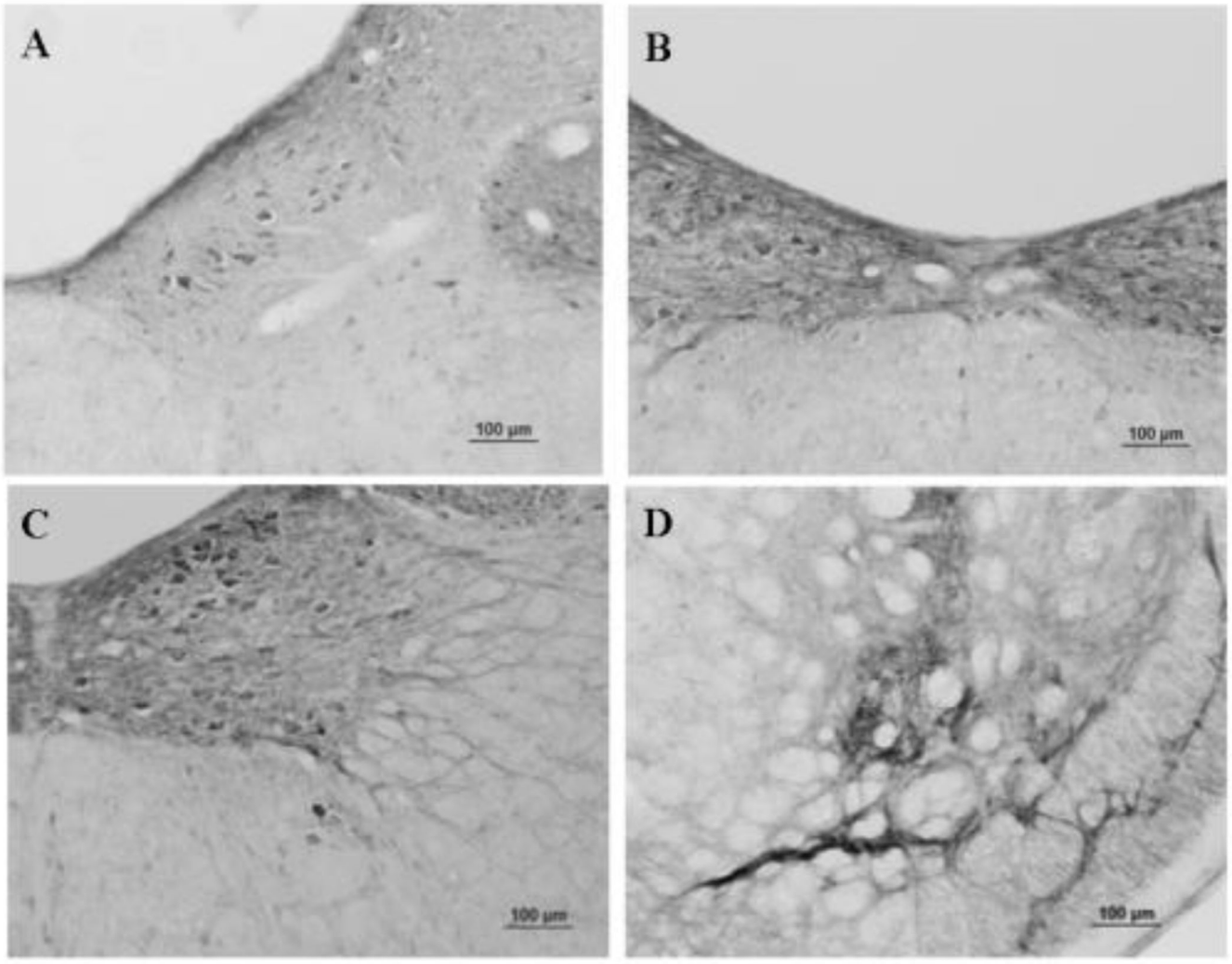

Figure 8.
Moderate expression of TRPV2 in low magnification images of the medial vestibular nucleus and rostral NTS (A), caudal aspect of the pontine nucleus (B), laterotegmental nucleus (C) and the lateral reticular nucleus (D). Scale bar = 100 µm in all the images.

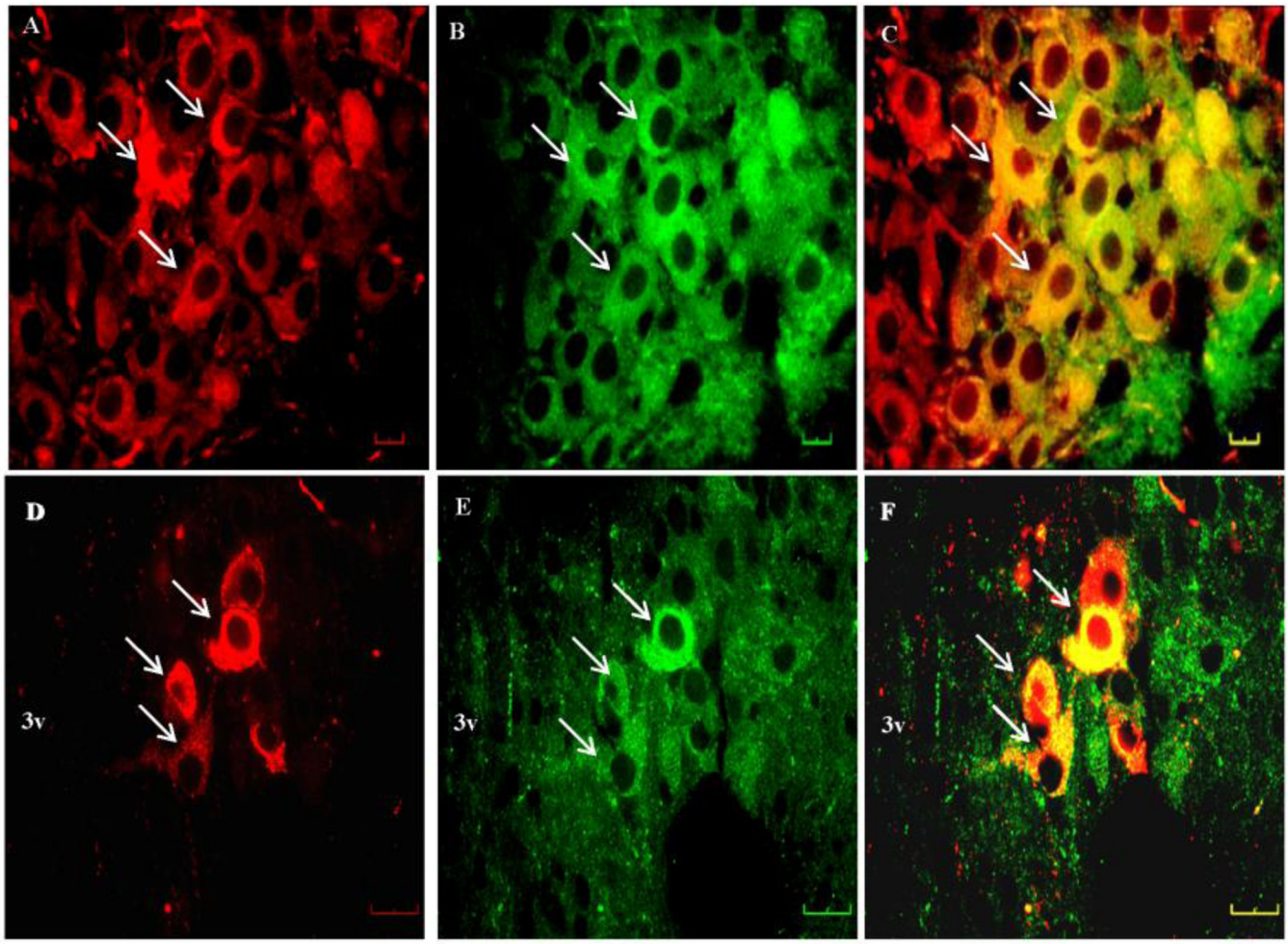

Figure 9.

High magnification images of TRPV2 colocalization with AVP in the SON (A–C) and PVN (D–F). These confocal images of densely Cy2 (green) labeled TRPV2 (B & E) colocalize with Cy3 (red) labeled AVP (A & D) in the SON and PVN. Neurons with TRPV2 and AVP colocalization are shown as yellow. Scale bar = 10 μm for all the images.

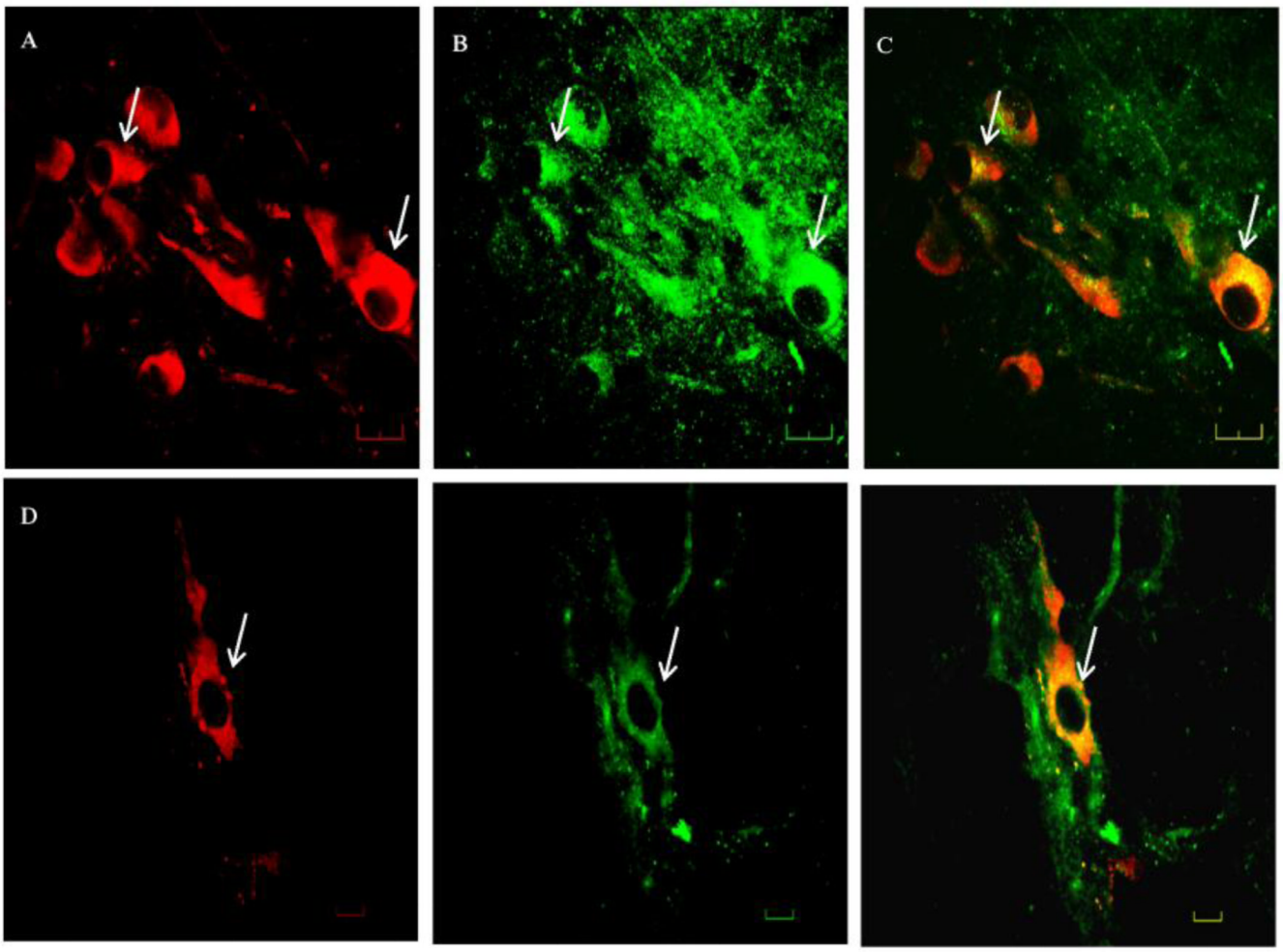

Figure 10.
High magnification images of TRPV2 colocalization with DBH in the NTS (A–C) and VLM (D–F). These confocal images of densely Cy2 (green) labeled TRPV2 (B & E) colocalize with Cy3 (red) labeled DBH (A & D) in the NTS and VLM. Neurons demonstrating colocalization are shown as yellow. Scale bar = 10 μm for all the images.

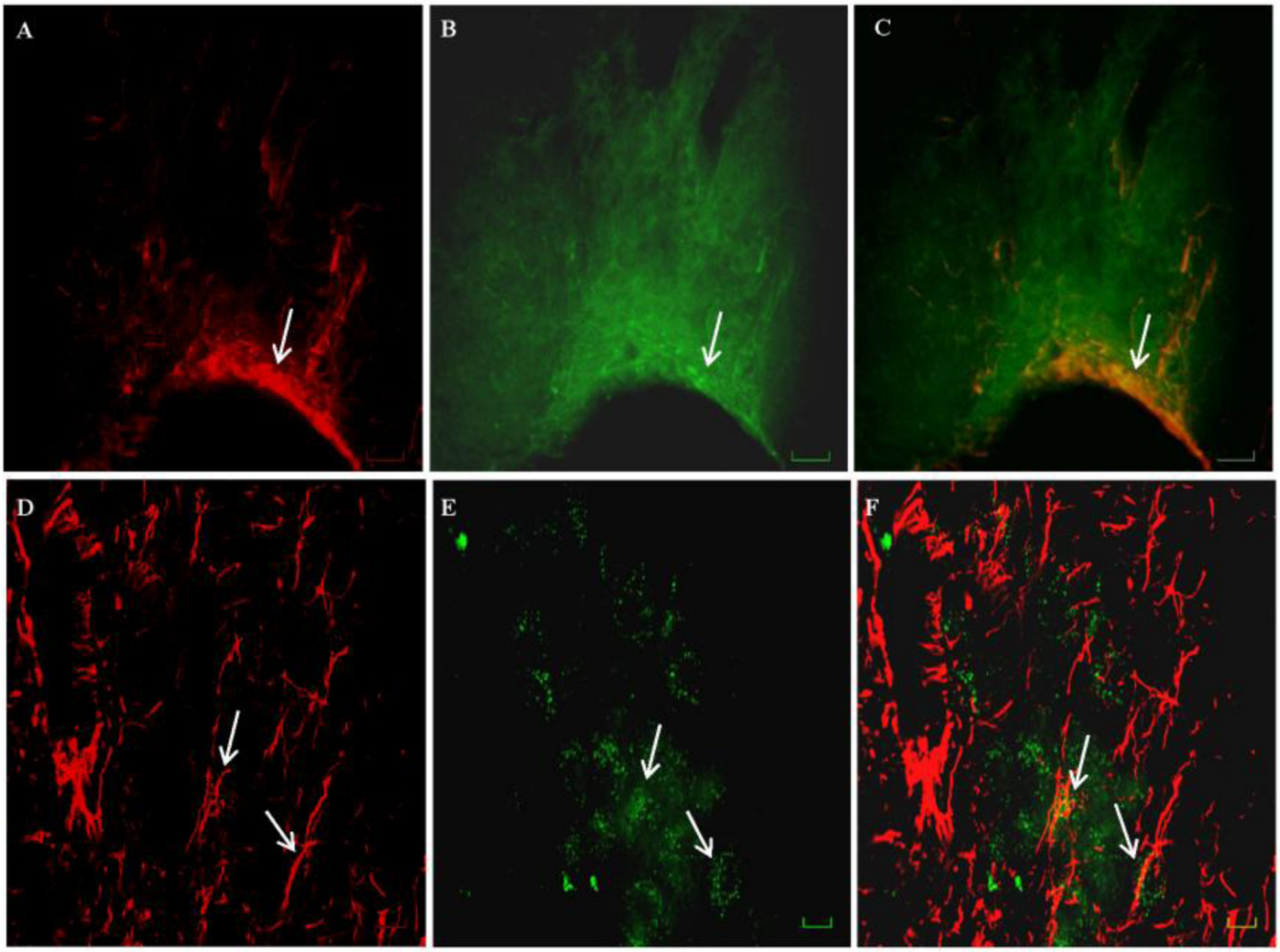

Figure 11.
Images of TRPV2 immunostaining with GFAP stained astrocyte processes in the SON (A–C). 60x high magnification images of TRPV2/GFAP double immunolabeling in the SON (D–F). Confocal images of Cy3 (red) labeled GFAP (A, D) and Cy2 (green) labeled TRPV2 and merged images (C, F) in the SON. Scale bar = 100 μm for A–C and 20 μm for D–F.

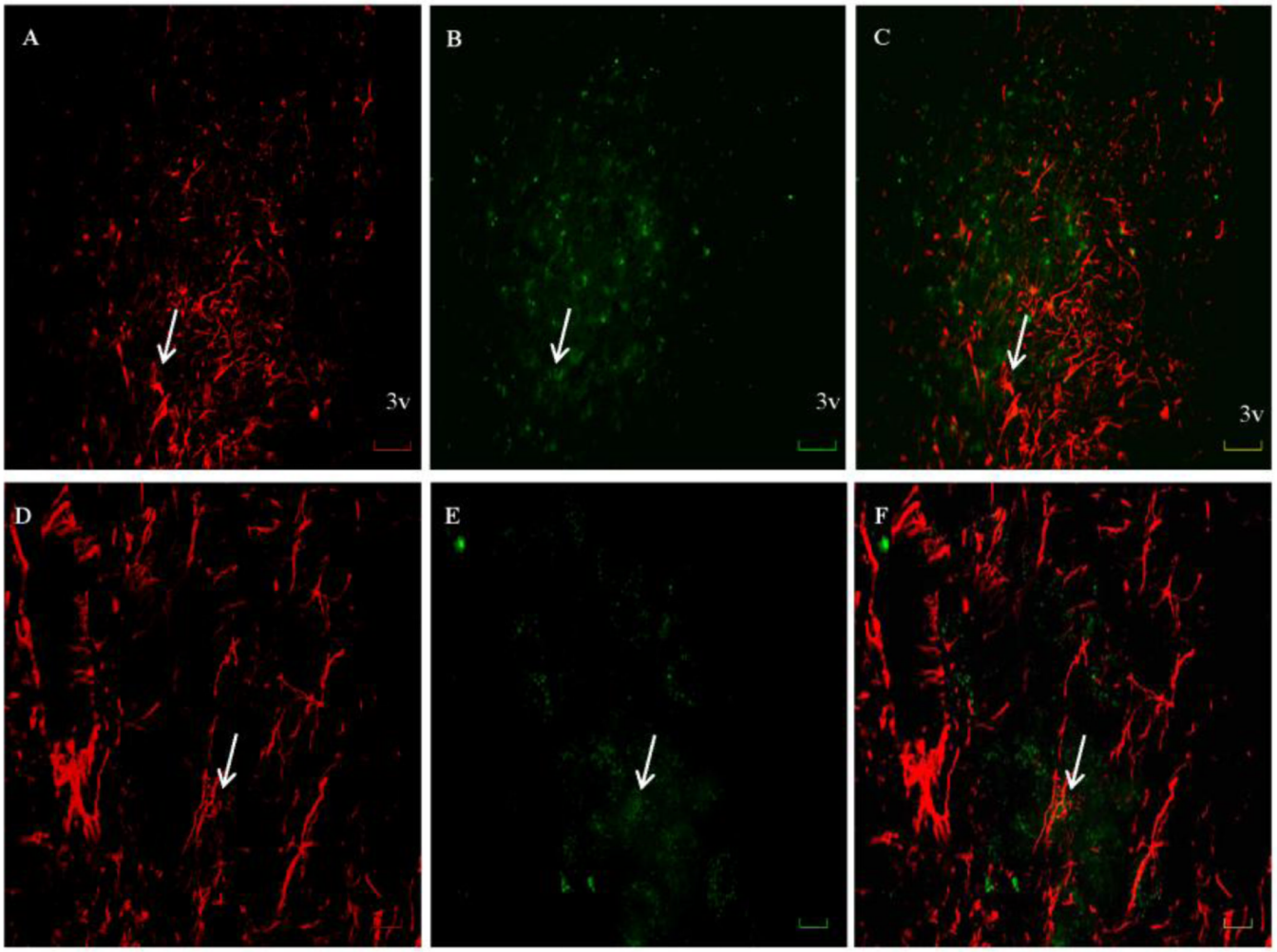

Figure 12.
Images of TRPV2 immunostaining with GFAP in the ARH (A–C) and the MFB (D–F). Confocal images of Cy3 (red) labeled GFAP (A, D) and Cy2 (green) labeled TRPV2 and merged images (C, F) in the ARH and MFB. 3v represents the third ventricle. Scale bar = 20 μm for all images.

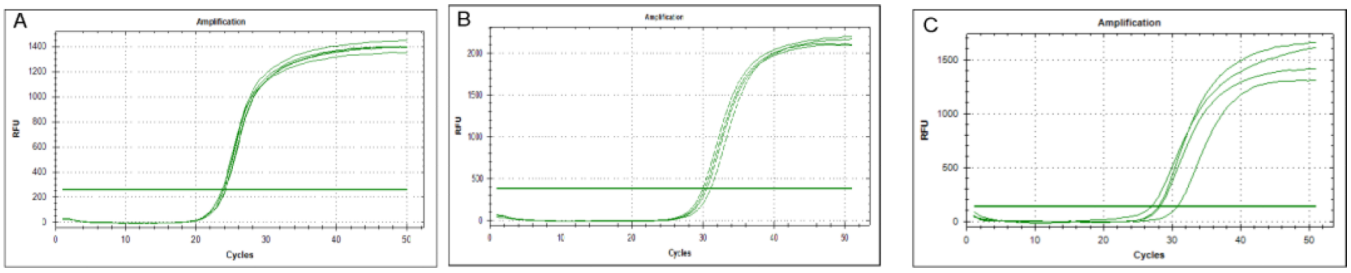

Figure 13.
Amplification curves for GAPDH (A), TRPV2 (B) and AVP (C) obtained by qRT-PCR from laser capture microdissected AVP neurons in the SON.

Table 1

Real-Time Quantitative-Reverse Transcriptase Polymerase Chain Reaction Primer Sequences

Primer sequences of the different genes of interest. The $2^{-\Delta CT}$ is calculated by subtracting the individual CT value of housekeeping gene (GAPDH) from the corresponding CT value of genes of interest

AVP forward primer:	5'- TGCCTGCTACTTCCAGAACTGC-3’
AVP reverse primer:	5'-AGGGGAGACACTGTCTCAGCTC-3’
TRPV2 sense primer:	5’-GAGTCACCATTCCAGAGGGA-3’
TRPV2 antisense primer:	5’-GTTCAGCACAGCCTTCATCA-3’
GAPDH forward primer:	5’-CTCATGACCACAGTCCATGC -3’
GAPDH reverse primer:	5’-TACATTGGGGGTAGGAACAC -3’

Table 2
Qualitative estimates of TRPV2-ir in the rat forebrain

Qualitative estimates of TRPV2 positive cells in regions of the rat forebrain.

Forebrain Regions	TRPV2-IR cells
Medial Forebrain Bundle	+
Supraoptic Nucleus	++++
Paraventricular nucleus rostral (magnocellular)	++
Paraventricular nucleus caudal (magnocellular)	+++
Paraventtricular nucleus (dorsal horn and posterior parvocellular)	++
Suprachiasmatic Nucleus	–
Retrochiasmatic Nucleus	+
Arcuate Nucleus of the Hypothalamus	++
Ventromedial hypothalamic nucleus	–
Dorsomedial hypothalamic nucleus	–
Median Eminence	+
Periventricular area	+
Lateral hypothalamic area	–
Medial Preoptic Nucleus	+
Organum vasculosum of lamina terminalis	+++
Bed Nucleus of Stria Terminalis	+
Anterior Amygdaloid Area- Ventral	++
Caudate Putamen	++
Cingulate cortex	+
HLFL cortex	+
Posterior hypothalamic area	–

Table 3
Qualitative estimates of TRPV2 in the rat hindbrain

Qualitative estimates of TRPV2 positive cells in regions of the rat hindbrain.

Hindbrain Regions	TRPV2-IR cells
Area Postrema	+
Hypoglossal Nucleus	+++
Nucleus of the solitary tract-medial, lateral and caudal	+++
C2 adrenaline cells	++
Locus Cereolus	+++
Inferior olive, subnucleus C of medial nucleus	++
Inferior olive, cap of kooy of the medial nucleus	++
Laterodorsal tegmental nucleus	++
Probst bundle	++
Pontine Nucleus Caudal	++
Lateral reticular nucleus	++
Raphae Magnus Nucleus	++
Raphae Pallidus nucleus	+
Rostroventrolateral reticular nucleus	+++
Caudoventrolateral reticular nucleus	+++
Sphenoid Nucleus	++
Sub Cereolus Ventral	++

Table 4

Quantitative estimates of TRPV2/AVP cells and TRPV2/DBH cells in the SON and NTS respectively.

Hypothalamic SON AVP/TRPV2 counts			Hindbrain NTS DBH/TRPV2 counts		
AVP	**TRPV2**	**Number of AVP cells that are TRPV2 +**	**DBH**	**TRPV2**	**Number of DBH cells that are TRPV2 +**
65 ± 8.34	75.25 ± 9.83	49.25± 10.23	16.5 ± 3.12	12.75 ± 1.80	5.25 ± 0.75